Mechanical and Dielectric Relaxation Phenomena of Poly(ethylene-2,6-napthalene dicarboxylate) by Fractional Calculus Approach

M. E. Reyes-Melo,[1] J. J. Martínez-Vega,[2] C. A. Guerrero-Salazar,[1] U. Ortiz-Méndez[1]

[1]*Doctorado en Ingeniería de Materiales, Universidad Autónoma de Nuevo León, Pedro de Alba s/n, Cd. Universitaria, San Nicolás de los Garza, N.L. 66450, México*
[2]*Laboratoire de Génie Electrique de l'Université Paul Sabatier de Toulouse (CNRS-UMR 5003), 118 Route de Narbonne, Toulouse Cedex France*

Received 18 January 2006; accepted 4 May 2006
DOI 10.1002/app.24813
Published online in Wiley InterScience (www.interscience.wiley.com).

ABSTRACT: The mechanical and dielectric relaxation phenomena in PEN-films have been studied using fractional models. A mechanical fractional model for the description of dynamic modulus, $E^* = E' + iE''$, and a dielectric fractional model for the dynamic relative permittivity, $\varepsilon_r^* = \varepsilon_r' - i\varepsilon_r''$. These models takes into account three relaxation phenomena and the corresponding differential equations have derivatives of fractional order between 0 and 1. In applying the Fourier transform to fractional differential equations and in considering that each relaxation mode is associated to cooperative or noncooperative molecular movements, we calculated $E^*(i\omega,T)$ and $\varepsilon_r^*(i\omega,T)$. The isochronal diagrams of the real and imaginary parts of either E^* and ε_r^* obtained from fractional models have been used to study the three relaxation phenomena (α, β*, and β) of poly (ethylene-2,6-napthalene dicarboxylate). An agreement between experiments and fractional models has been achieved for both mechanical and dielectric relaxation phenomena, and the effect of morphology samples on the fractional order parameters of the Fractional Models are related to molecular motions associated to α, β*, and β relaxations. © 2006 Wiley Periodicals, Inc. J Appl Polym Sci 102: 3354–3368, 2006

Key words: relaxation; dielectric properties; mechanical properties; modeling; structure–property relations

INTRODUCTION

Poly(ethylene naphthalene-2,6-dicarboxylate) or PEN is a high performance thermoplastic polyester. The naphthalene groups in their repeat units (Fig. 1) gives a stronger rigidity to their macromolecular chains, consequently PEN has a combination of good thermal stability, degradation resistance, good mechanical and dielectric properties, low dielectric loss factor, and low permeability.[1–3]

PEN can be obtained as very thin (1 μm) films at reasonable cost, and gives response to high demanding mechanical and electrical engineering requirements as insulator or dielectric material in electrical or electronic and other engineering applications.[3]

In general, the properties of PEN have a viscoelastic behavior and depend strongly on the morphology of the sample. The morphology of PEN-films is an intimate mixture of ordered crystals and amorphous phase that give rise to a complex semicrystalline structure, and their applications require a thorough knowledge of the relaxation phenomena that these materials can undergo. The relaxation phenomena are associated with molecular mobility leading to a new structural equilibrium with low energy content.

Several experimental works on PEN samples show that both dynamic mechanical analysis (DMA) and dielectric relaxation spectroscopy (DRS) display at least three relaxation phenomena.[4–8] In order of decreasing temperature: the α-relaxation, which is associated to cooperative movements of chain segments reflecting the glass transition process, the β*-process, which is associated to partially cooperative motions assigned to naphthalene groups,[1,6–8] and the β-relaxation due to local fluctuations of the carbonyl groups. These molecular motions reflect the rate at which a portion of energy has been lost. This makes a very difficult analysis of the polymer properties using the traditional calculus, and in this sense, Fractional Calculus is an alternative to describe the relaxation phenomena.[9–13] Fractional calculus is the branch of mathematics that deals with the generalization of integrals and derivatives to all real (and even complex) orders.[9,11] In the case of relaxation phenomena, the noninteger order of a fractional integral is an indication of the remaining or preserved energy of a signal passing

Correspondence to: M. E. Reyes-Melo (mreyes@fime.uanl.mx).

Contract grant sponsors: ECOS (France), ANUIES (Mexico), UANL (Mexico).

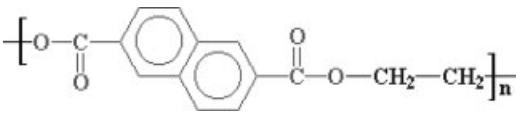

Figure 1 Repeat unit structure of poly(ethylene-2,6-naphthalene dicarboxylate).

trough a system with partial energy dissipation.[11,14] Similarly, the fractional order of a differentiation reflects the rate at which a portion of the energy has been lost.

The aim of this study is a fractional calculus approach to the mechanic and dielectric manifestations of the viscoelasticity of PEN over a wide temperature range, from glassy to glass transition region. In addition, the effect of morphology samples on the parameters of the fractional models is also studied.

FRACTIONAL CALCULUS AND THE VISCOELASTIC BEHAVIOR OF POLYMER MATERIALS

In recent years, there has been a considerable amount of work carried out on the application of the fractional calculus method to modeling the viscoelastic response (mechanical and dielectric relaxations) of polymer materials,[12–20] over a wide range of temperature (T) and time (t) or frequency (ω).

In the case of mechanical relaxation phenomena (the mechanic manifestation of viscoelasticity), the fractional calculus method uses the idea that the spring and dashpot elements in the rheological models can be replaced by a ''spring-pot'' element. This new rheological element called ''spring-pot'' (Fig. 2) combines the solid behavior (Hooke's law) with fluid behavior (Newton's law).[9,10,14,16–18]

$$\sigma = E^{1-b}\eta^{b}D_t^b S = E\left(\frac{\eta}{E}\right)^{b} D_t^b S = E\tau^b D_t^b S \qquad (1)$$

where σ is the stress, S is the deformation, E is the elastic modulus, η is viscosity, $\tau = \eta/E$ is a characteristic time called relaxation time, which could be to associated to time required by segments chains in movement for a complete reorganization and a full reorientation to a new structural equilibrium state, and $D_t^b S$ is the derivative of b order ($0 \leq b \leq 1$) of the deformation with respect to time:

$$D_t^b S = \frac{1}{\Gamma(1-b)}\frac{d}{dt}\int_0^t (t-y)^{-b} S(y)dy \qquad (2)$$

where Γ is the Gamma function:

$$\Gamma(x) = \int_0^\infty \left(e^u u^{x-1}\right) du \quad \text{with} \quad x > 0 \qquad (3)$$

From eq. (1), one obtains the Hooke's law or spring behavior when $b = 0$, and when $b = 1$, one obtains the Newtons's law or dashpot behavior (Fig. 2).

Schiessel and Blumen,[21] Heymans and Bauwens[22] have demonstrated that the differential equation of the spring-pot element can be realized physically through hierarchical arrangements of springs and dashpots, such as ladders, trees, and fractal networks. Hilfer[23] has also found that fractional time derivatives of order between 0 and 1 arise naturally in the transition between microscopic and macroscopic time scales. It has been shown that constitutive equations employing derivatives of fractional order are linked to molecular theories describing the macroscopic behavior of viscoelastic materials as polymers.[14–20]

On the other hand, for the dielectric manifestation of viscoelasticity, Hilfer[23] published several papers concerning the fractional calculus method and its application to fitting the dielectric data of glass forming liquids and of propylene carbonate. In these works, Hilfer introduced a novel fitting function for the complex frequency-dependent dielectric susceptibility, this fitting function contains a single stretched exponent, similar to the empirical Cole-Davison equation or the Kohlraush-Williams-Watt stretched exponential fits. The physical and geometrical interpretation of fractional order of the differential and integral operators has been studied by Moshrefi-Torbati,[11] he used fractional operators to define the relationship between electrical current and voltage for an electronic circuit that consist of a domino ladder network of a chain of resistors and a chain of capacitors interconnected at each node, in physics terms, a capacitor stores energy and a resistor dissipates energy, in the domino ladder, this happens at each node, consequently the ratio of the stored and dissipated energy in all electronic circuit can be controlled by varying the values of the fractional order used, which depend of the resistance values in the resistor chains and of the capacitance values in the capacitor chain. More recently, Reyes-Melo et al.[14,19,20] have used Fractional Calculus to obtain a fractional differential equation

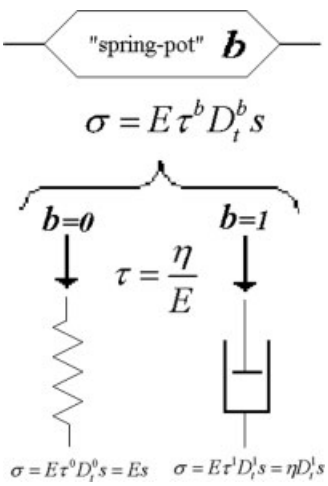

Figure 2 The ''spring-pot'' element.

relating the electrical stress, V, and the electrical current, I:

$$V = \left(\frac{1}{C}\right)^{1-a} R^a D_t^a Q = \frac{(RC)^a}{C} D_t^a Q = \frac{\tau^a}{C} D_t^a Q \quad (4)$$

In eq. (4), R is the electrical resistance, C is the capacitance, and $D_t^a Q$ is the fractional derivative of electrical charge, Q, with respect to time with evidently $0 \leq a \leq 1$, and $RC = \tau$ is a characteristic time called relaxation time, which could be to associated with the time required by chain segments (electrical-dipoles) in movement for a complete reorganization and a full reorientation to a new state of structural equilibrium. Equation 4 represents a new electrical-fractional element named ''cap-resistor.'' From eq. (4), the electrical resistance behavior is obtained when $a = 1$, and when $a = 0$, the electric behavior is that of a capacitor (Fig. 3).

In the following section, we used spring-pots and cap-resistors elements to obtain the mechanical fractional model (MFM) and the dielectric fractional model (DFM) for mathematical descriptions of the mechanical and dielectric relaxation phenomena of PEN. For mechanical relaxation phenomena, it is necessary to describe the dynamic modulus, $E^* = E' + iE''$. In the case of dielectric relaxation phenomena, it is necessary a mathematical description of the complex relative permittivity, $\varepsilon_r^* = \varepsilon_r' - i\varepsilon_r''$.

FRACTIONAL CALCULUS MODELING OF THE DYNAMIC ELASTIC MODULUS, E^*, AND THE RELATIVE COMPLEX DIELECTRIC PERMITTIVITY, ε^*

The classical models to describe mechanical and dielectric properties in polymer systems are based using arrangements of ideal (rheological or electrical) elements. In the case of E^*, the rheological elements used are Hookean-springs and Newtonian-dashpots. Among these mechanical classics models, the simplest are those of Maxwell, Voigt-Kelvin, and Zener.

For ε_r^*, the electrical elements used are resistors and capacitors to build electrical circuits, as for example the classical Debye model. This model is analogous to classical Zener model used as a first approximation for the mathematical description of E^* characterized by only one relaxation phenomenon. It is important to remark here which the Zener model is described with the same formalism as the Debye model, with the correspondence $E \Leftrightarrow \frac{1}{C}$, $\eta \Leftrightarrow R$, $S \Leftrightarrow Q$, and $\sigma \Leftrightarrow V$.

Unfortunately, these classical models are not appropriated to represent the experimental data of E^* and ε_r^* of semicrystalline polymers as PEN-films. However, a better mathematical description of E^* and ε_r^* can be obtained by replacing classical elements for the new fractional elements in the classical models.[14,16,18–20]

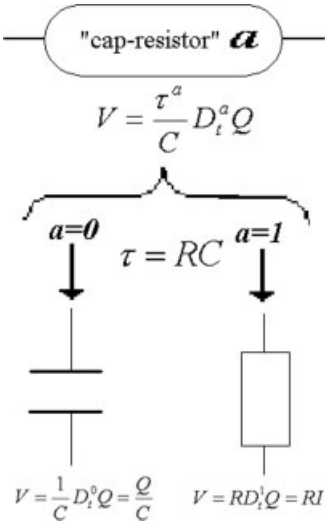

Figure 3 The ''cap-resistor'' element.

Mechanical fractional model

For modeling the mechanic manifestation of viscoelasticity of PEN we developed a mechanical fractional model (MFM) based on three fractional Zener models[14,18] arranged in parallel (Fig. 4). The first one posses two spring-pots: a and b, associated mainly with α-mechanic relaxation. The second one has only one spring-pot c, and it is associated with β*-mechanic relaxation. The last one also has only one spring-pot d, associated with the mechanic manifestation of β.

In DMA, the polymer is subject to an alternating strain, S, measuring the resulting stress, σ. Because of viscoelasticity, S and σ are out of phase an angle $0 < \delta < \pi/2$, consequently they can be written as complex numbers in the following way:

$$\begin{aligned} S^* &= S_0 \exp(i\omega t) \qquad \sigma^* = \sigma_0 \exp(i\omega t + \delta) \\ \sigma^* &= E^* S^* \end{aligned} \quad (5)$$

where ω is the angular frequency, and $E^* = E' + iE''$ is the complex modulus. Applying the Fourier transform to the global stress, σ, of the MFM and considering which the global deformation, S, is equal to individual deformations of each element of the MFM, we obtain that the complex modulus is defined by:

$$\begin{aligned} E^* &= E1^* + E2^* + E3^* \\ &= (E1' + iE1'') + (E2 + iE2'') + (E3' + iE3'') \end{aligned} \quad (6)$$

Consequently, the individual complex modulus: $E1^*$, $E2^*$, and $E3^*$ were calculated separately from elements 1, 2, and 3, respectively.[14,18]

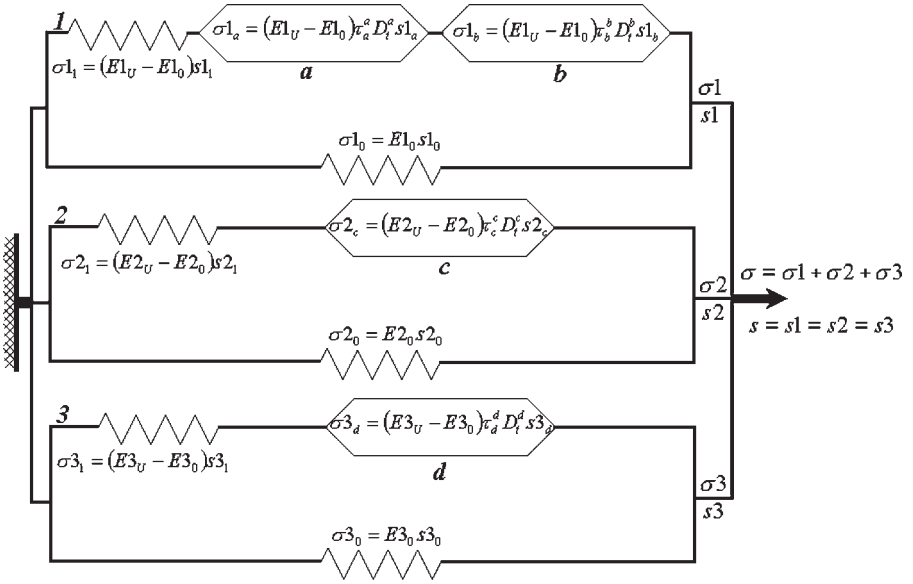

Figure 4 The mechanical fractional model (MFM) for modeling the mechanic manifestations of α, β*, and β relaxations of PEN.

The real, $E1'$, and imaginary, $E1''$, parts of $E1^*$ are defined by:

$$\left.\begin{aligned} E1' &= E1_0 + \frac{(E1_U - E1_0)(1 + A_1)}{(1 + A_1)^2 + A_2^2} \\ E1'' &= \frac{(E1_U - E1_0)A_2}{(1 + A_1)^2 + A_2^2} \end{aligned}\right\} \left.\begin{aligned} A_1 &= [\omega\tau_b]^{-b} \cos\left(b\frac{\pi}{2}\right) + [\omega\tau_a]^{-a} \cos\left(a\frac{\pi}{2}\right) \\ A_2 &= [\omega\tau_b]^{-b} \sin\left(b\frac{\pi}{2}\right) + [\omega\tau_a]^{-a} \sin\left(a\frac{\pi}{2}\right) \end{aligned}\right\} \tag{7}$$

For element 2, $E2'$ and $E2''$ are defined by:

$$\left.\begin{aligned} E2' &= E2_U - \frac{(E2_U - E2_0)(1 + B_1)}{(1 + B_1)^2 + B_2^2} \\ E2'' &= \frac{(E2_U - E2_0)B_2}{(1 + B_1)^2 + B_2^2} \end{aligned}\right\} \left.\begin{aligned} B_1 &= (\omega\tau_c)^c \cos\left(c\frac{\pi}{2}\right) \\ B_2 &= (\omega\tau_c)^c \sin\left(c\frac{\pi}{2}\right) \end{aligned}\right\} \tag{8}$$

And for element 3, $E3'$ and $E3''$ are defined by:

$$\left.\begin{aligned} E3' &= E3_U - \frac{(E3_U - E3_0)(1 + C_1)}{(1 + C_1)^2 + C_2^2} \\ E3'' &= \frac{(E3_U - E3_0)C_2}{(1 + C_1)^2 + C_2^2} \end{aligned}\right\} \left.\begin{aligned} C_1 &= (\omega\tau_d)^d \cos\left(d\frac{\pi}{2}\right) \\ C_2 &= (\omega\tau_d)^d \sin\left(d\frac{\pi}{2}\right) \end{aligned}\right\} \tag{9}$$

From eqs. (6)–(9), we obtain the mathematical expressions for E' and E'':

$$E' = E1' + E2' + E3' = E1_0 + \frac{(E1_U - E1_0)(1 + A_1)}{(1 + A_1)^2 + A_2^2} + E2_U - \frac{(E2_U - E2_0)(1 + B_1)}{(1 + B_1)^2 + B_2^2} + E3_U - \frac{(E3_U - E3_0)(1 + C_1)}{(1 + C_1)^2 + C_2^2} \tag{10}$$

$$E'' = E1'' + E2'' + E3''$$
$$= \frac{(E1_U - E1_0)A_2}{(1+A_1)^2 + A_2^2} + \frac{(E2_U - E2_0)B_2}{(1+B_1)^2 + B_2^2} + \frac{(E3_U - E3_0)C_2}{(1+C_1)^2 + C_2^2} \tag{11}$$

Theoretical predictions of the frequency[14] and temperature[14,18] dependence of E' and E'' can be obtained from eqs. (10) and (11).

Dielectric fractional model

In the case of the dielectric behavior of PEN, the dielectric fractional model (DFM) is based on three electrical circuits, arranged in parallel (Fig. 5). The first one possesses two cap-resistors: *e* and *f*, and they are mainly associated to α-dielectric relaxation. The second one has only one cap-resistor, *g*, and it is associated with dielectric manifestation of β*-relaxation. The last one also has only one cap-resistor, *h*, associated with β-dielectric relaxation.

In the DFM, the electric charge, Q, is the result of the contributions of elements: 1, 2, and 3, and the voltage, V, is equal to individual voltage of each element. Under a sinusoidal alternating voltage applied at an angular frequency ω, the voltage and electric current, I, are out of phase an angle $0 < \theta < \pi/2$, consequently, V, I, and the admittance, Y, can be written as a complex numbers in the following way:

$$V^* = V_0 \exp(i\omega t) \qquad I^* = I_0 \exp(i\omega t + \theta) \qquad Y^* = \frac{I^*}{V^*} \tag{12}$$

From the determination of the admittance Y^* and using eq. (13), we can estimate in a first approximation the complex capacity, C^*, or the relative complex dielectric permittivity, ε_r^*:

$$\varepsilon_r^* = \frac{\varepsilon^*}{\varepsilon_0} = \frac{C^*}{C_0} = \frac{Y^*}{i w C_0} \tag{13}$$

Applying the Fourier transform to Q and V of the DFM and using eq. (13) and $\varepsilon_r^* = \varepsilon_r' - i\varepsilon_r''$, we obtain that ε_r^* could be expressed as a function of the corresponding relative complex permittivity of each element of our DFM:

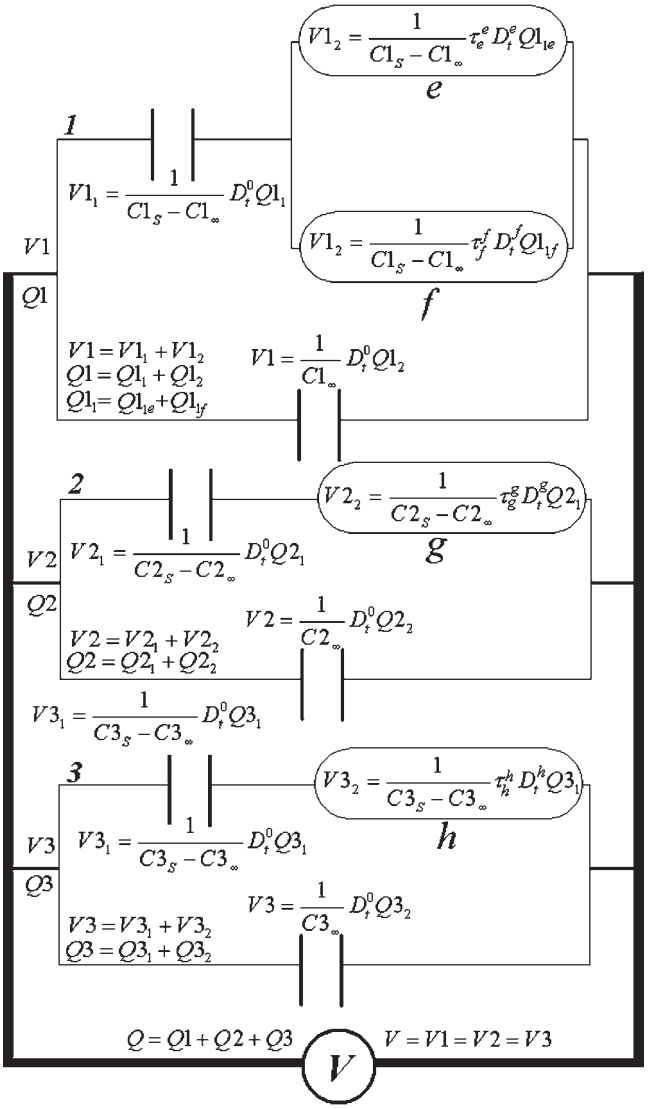

Figure 5 The dielectric fractional model (DFM) for the mathematical description of α, β*, and β dielectric relaxations of PEN.

$$\varepsilon_r^* = \varepsilon 1_r^* + \varepsilon 2_r^* + \varepsilon 3_r^*$$
$$= (\varepsilon 1_r' - i\varepsilon_r'') + (\varepsilon 2_r' - i\varepsilon 2_r'') + (\varepsilon 3_r' - i\varepsilon 3_r'') \tag{14}$$

The individual complex permittivities: $\varepsilon 1_r^*$, $\varepsilon 2_r^*$, and $\varepsilon 3_r^*$ were calculated separately from elements 1, 2, and 3, respectively.[14,19,20]

The real, $\varepsilon 1_r'$ and imaginary, $\varepsilon 1_r''$, parts of $\varepsilon 1_r^*$ are:

$$\left.\begin{aligned} \varepsilon 1_r' &= \varepsilon 1_{rs} - \frac{(\varepsilon 1_{rs} - \varepsilon 1_{r\infty})(1+F_1)}{(1+F_1)^2 + F_2^2} \\ \varepsilon 1_r'' &= \frac{(\varepsilon 1_{rs} - \varepsilon 1_{r\infty})F_2}{(1+F_1)^2 + F_2^2} \end{aligned}\right\} \quad \left.\begin{aligned} F_1 &= (\omega\tau_e)^{-e}\cos\left(e\frac{\pi}{2}\right) + (\omega\tau_f)^{-f}\cos\left(f\frac{\pi}{2}\right) \\ F_2 &= (\omega\tau_e)^{-e}\sin\left(e\frac{\pi}{2}\right) + (\omega\tau_f)^{-f}\sin\left(f\frac{\pi}{2}\right) \end{aligned}\right. \tag{15}$$

For element 2 of our DFM, $\varepsilon 2'_r$ and $\varepsilon 2''_r$ are defined by:

$$\left.\begin{aligned}\varepsilon 2'_r &= \varepsilon 2_{r\infty} + \frac{(\varepsilon 2_{rs} - \varepsilon 2_{r\infty})(1+G_1)}{(1+G_1)^2+G_2^2} \\ \varepsilon 2''_r &= \frac{(\varepsilon 2_{rs} - \varepsilon 2_{r\infty})G_2}{(1+G_1)^2+G_2^2}\end{aligned}\right\} \begin{aligned} G_1 &= (\omega\tau_g)^g \cos\left(g\frac{\pi}{2}\right) \\ G_2 &= (\omega\tau_g)^g \sin\left(g\frac{\pi}{2}\right)\end{aligned} \tag{16}$$

And finally for element 3, $\varepsilon 3'_r$ and $\varepsilon 3''_r$ are defined by:

$$\left.\begin{aligned}\varepsilon 3'_r &= \varepsilon 3_{r\infty} + \frac{(\varepsilon 3_{rs} - \varepsilon 3_{r\infty})(1+H_1)}{(1+H_1)^2+H_2^2} \\ \varepsilon 3''_r &= \frac{(\varepsilon 3_{rs} - \varepsilon 3_{r\infty})H_2}{(1+H_1)^2+H_2^2}\end{aligned}\right\} \begin{aligned} H_1 &= (\omega\tau_f)^f \cos\left(f\frac{\pi}{2}\right) \\ H_2 &= (\omega\tau_f)^f \sin\left(f\frac{\pi}{2}\right)\end{aligned} \tag{17}$$

From eqs. (14)–(17), we obtain the mathematical expressions for ε'_r and ε''_r:

$$\varepsilon'_r = \varepsilon 1'_r + \varepsilon 2'_r + \varepsilon 3'_r = \varepsilon 1_{rs} - \frac{(\varepsilon 1_{rs} - \varepsilon 1_{r\infty})(1+F_1)}{(1+F_1)^2+F_2^2} + \varepsilon 2_{r\infty} + \frac{(\varepsilon 2_{rs} - \varepsilon 2_{r\infty})(1+G_1)}{(1+G_1)^2+G_2^2} + \varepsilon 3_{r\infty} + \frac{(\varepsilon 3_{rs} - \varepsilon 3_{r\infty})(1+H_1)}{(1+H_1)^2+H_2^2} \tag{18}$$

$$\varepsilon''_r = \varepsilon 1''_r + \varepsilon 2''_r + \varepsilon 3''_r = \frac{(\varepsilon 1_{rs} - \varepsilon 1_{r\infty})F_2}{(1+F_1)^2+F_2^2} + \frac{(\varepsilon 2_{rs} - \varepsilon 2_{r\infty})G_2}{(1+G_1)^2+G_2^2} + \frac{(\varepsilon 3_{rs} - \varepsilon 3_{r\infty})H_2}{(1+H_1)^2+H_2^2} \tag{19}$$

Theoretical predictions of the frequency and temperature dependence of ε'_r and ε''_r can be obtained from eqs. (18) and (19).[14,20]

In the practice, it is must easy and very useful the analysis of the temperature dependence of E^* and ε^* to a constant frequency (isochronal conditions) that the analysis of the frequency dependence to a constant temperature (isothermal conditions). So, it is necessary obtain isochronal descriptions of E^* and ε^* from MFM and DFM respectively.

Isochronal response of MFM and DFM

To obtain the temperature dependence of the real and imaginary parts of either E^* and ε^*, we need to define the relationship between τ parameters and temperature, T, which in turn depends of cooperative and noncooperative nature of the molecular motions associated to each τ parameter of the MFM and the DFM. The molecular mobility associated to β-relaxation is noncooperative. For β^*-relaxation, the movements are partially cooperative, and finally α-relaxation is associated to cooperative motions.

The relaxation time, $\tau(T)$, for noncooperative motions (β-relaxation) follows an Arrhenius law behavior:

$$\tau(T) = \tau_0 \exp\left(\frac{E_a}{k_B T}\right) \tag{20}$$

In eq. (20), the activation energy, E_a, could have magnitudes that are identifiable with real energy barriers, k_B is the Boltzmann constant, T is the absolute temperature, and τ_0 is the pre-exponential factor and typically it falls within the range $10^{-16}\ s \le \tau_0 \le 10^{-13}\ s$; values of τ_0 in the vicinity of the upper limit correspond to molecular vibrational times and the lower limit may be rationalized by and additional entropy contributions.[24]

On the other hand, cooperative motions involve simultaneous movements of segments chains. The probability success for cooperative motions is P^Z, being $P \propto 1/\tau$ the probability of a single elementary movement, and Z exponent can be considered as the number of elementary movements, consequently, $\tau_{\text{cooperative}}$ verify a power law.[25]

$$\tau_{\text{cooperative}}(T) = \tau_0 \left(\frac{\tau}{\tau_0}\right)^Z = \tau_0 \left[\exp\left(\frac{E_a}{k_B T}\right)\right]^Z \qquad T_0 \le T \le T^* \tag{21}$$

In eq. (21), τ is the relaxation time of the elementary movement defined by an Arrhenius behavior, and Z exponent is dependent of polymer structure and it is calculated with the next equation:[14,25]

$$Z(T) = \frac{T}{T^*}\frac{T^* - T_0}{T - T_0} \qquad T_0 \le T \le T^* \tag{22}$$

Above a crossover temperature, T^*, cooperative and noncooperative movements merge together[25] and $Z = 1$, below T^* the relaxation times of cooperative movements verify the empirical Vogel-Fulcher-Tammann equation, this temperature T^* is of the order of 1.3 T_g in polymers completely amorphous and in semicrystalline polymers T^* is found equal to the melting temperature.[14,25] The relaxation time, τ^*, corresponding to T^* has been reported of the order of 10^{-7}–10^{-9} s for several polymers.[25] T_0 is a temperature below T_g where Z and $\tau_{\text{cooperative}}$, extrapolates to infinity.

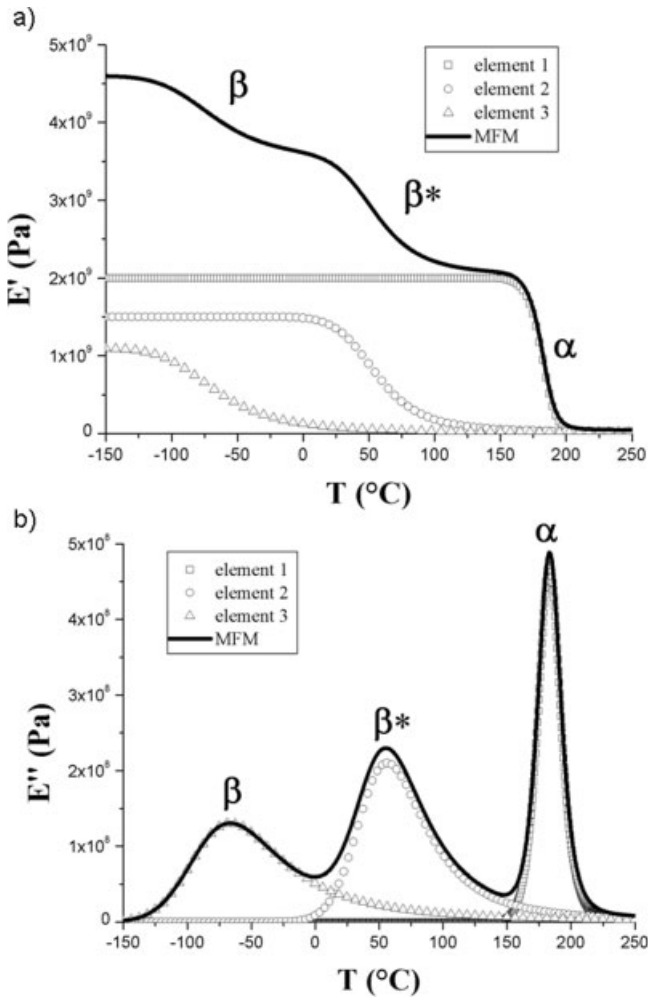

Figure 6 Predictions of the real (a), and imaginary parts (b) of E^* under isochronal conditions to $f = 10$ Hz. Parameters for element 1: $a = 0.4$, $b = 0.8$, $E1_U = 2 \times 10^9$ Pa, $E1_0 = 1 \times 10^7$ Pa, $\tau_b(T) = \tau_a(T)$, $\tau_0 = 1 \times 10^{-14}$ s, $E_{a\ \text{single-movement}} = 0.75$ eV , $T^* = 540$ K, $T_0 = 350$ K. Parameters for element 2: $c = 0.35$, $E2_U = 1.5 \times 10^9$ Pa, $E2_0 = 1.1 \times 10^7$ Pa, $\tau_0 = 1 \times 10^{-14}$ s, $E_{a\ \text{single-movement}} = 0.6$ eV, $T^* = 540$ K, $T_0 = 150$ K. Parameters for element 3: $d = 0.3$, $E3_U = 1.1 \times 10^9$ Pa, $E3_0 = 1.2 \times 10^7$ Pa, $\tau_0 = 1 \times 10^{-14}$ s, $E_{a\ \text{apparent}} = 0.5$ eV.

Figures 6(a and b) show the isochronal predictions of the real and imaginary parts of E^* obtained from the MFM (Fig. 4). The individual contributions of each element of MFM also are showed. The diagram of $E''(T)$ shows the existence of three peaks corresponding each one to mechanical relaxations. Each peak of $E''(T)$ is associated to an important variation on $E'(T)$ diagram. On $E''(T)$ diagram, the peak at a lower temperatures represents noncooperative movements (β-relaxation) and it is defined mainly for parameters of element 3 of the MFM, the second peak is associated to partially cooperative motions (β*-relaxation) and it is defined mainly for parameters of element 2, and the last one at higher temperatures is associated to cooperative movements (α-relaxation) and it is defined mainly by parameters of element 1.

On the other hand, Figure 7(a and b) show the isochronal predictions of the ε_r' and ε_r'' of ε_r^*, obtained from the DFM. The isochronal behavior of ε_r'' also shows three peaks but in this case each peak is associated to an important increases of $\varepsilon_r'(T)$ with increasing temperature. The peak at a lower temperatures represents noncooperative movements (β-relaxation) and it is defined mainly for parameters of electric-circuit 3 of the DFM, the second peak is associated to partially cooperative motions (β*-relaxation) and it is defined mainly for parameters of electric-circuit 2, and the last one at higher temperatures is associated to cooperative movements (α-

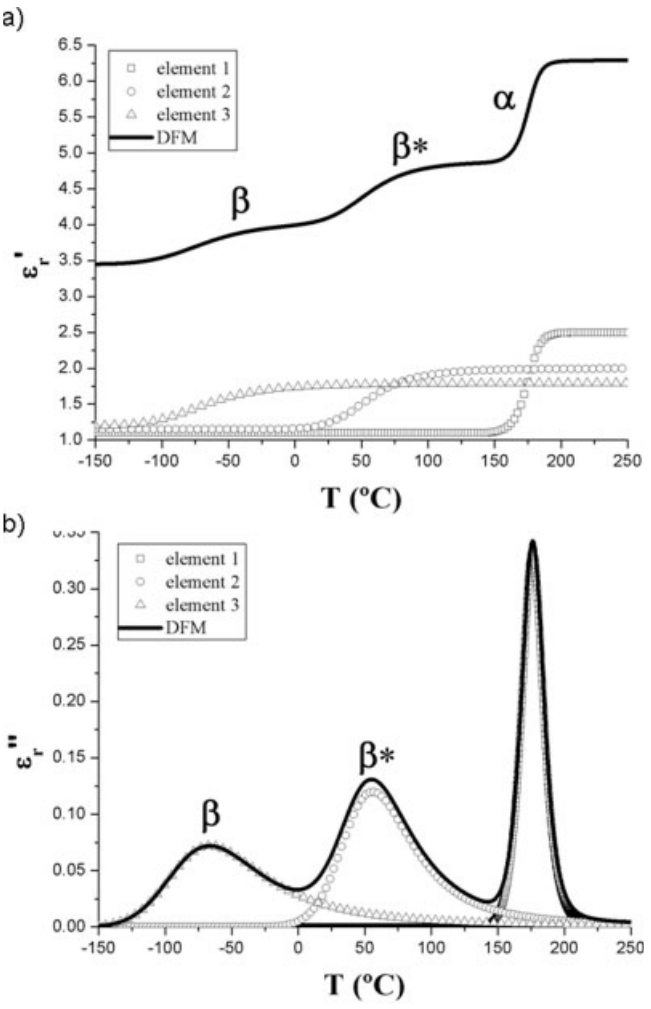

Figure 7 Predictions of the real (a), and imaginary (b) parts of ε_r^* under isochronal conditions to $f = 10$ Hz. Parameters for element 1: $e = 0.4$, $f = 0.8$, $\varepsilon 1_{rs} = 2.5$, $\varepsilon 1_{r\infty} = 1.1$, $\tau_e(T) = \tau_f(T)$, $\tau_0 = 1 \times 10^{-14}$ s, $E_{a\ \text{single movement}} = 0.7$ eV, $T^* = 540$ K, $T_0 = 350$ K. Parameters for element 2: $g = 0.35$, $\varepsilon 2_{rs} = 2$, $\varepsilon 2_{r\infty} = 1.15$, $\tau_0 = 1 \times 10^{-14}$ s, $E_{a\ \text{single-movement}} = 0.6$ eV, $T^* = 540$ K, $T_0 = 150$ K. Parameters for element 3: $h = 0.3$, $\varepsilon 3_{rs} = 1.8$, $\varepsilon 3_{r\infty} = 1.2$, $\tau_0 = 1 \times 10^{-14}$ s, $E_{a\ \text{apparent}} = 0.5$ eV.

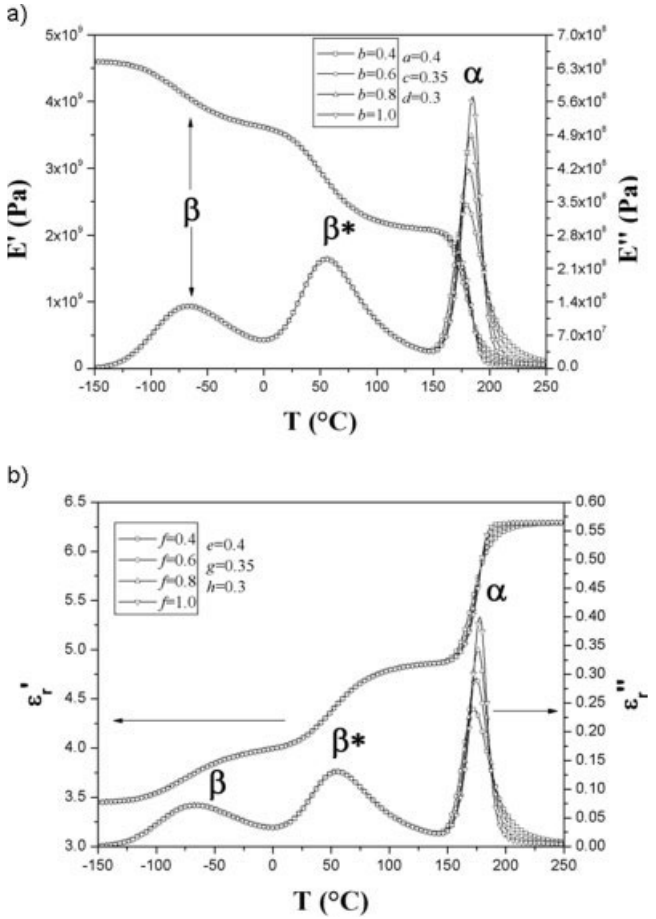

Figure 8 (a) Theoretical predictions of E' and E'' for different values of b, remaining a, c, and d constants. (b) Theoretical predictions of ε_r' and ε_r'' for different values of f, remaining e, g, and h constants.

relaxation) and it is defined mainly by parameters of electric-circuit 1.

The classical responses of E^* and ε_r^* for polymer materials having three relaxation phenomena can be obtained by choosing the values of the fractional orders of each model.[14,16,18–20] The shape of theoretical curves in Figures 6(a, b), 7(a and b) can be modified changing the values of the fractional orders of the spring-pots and the cap-resistors of each fractional model (MFM and DFM). The fractional orders a, b, c, and d in MFM and e, f, g and h in DFM can take values between 0 and 1. In Refs. 14, 18, and 20, we tested the viscoelastic response of MFM and DFM varying the fractional orders of the spring-pots in the MFM and the fractional orders of the cap-resistors in the DFM. Figure 8(a) shows the theoretical predictions of the loss (E'' versus T) and storage (E' versus T) modulus for different values of b, remaining a, c, and d constants; in this case, only the maximum of α is affected by changing the values of b. Figure 8(b) shows the isochronal predictions of ε_r' and ε_r'' for different values of f, and remaining e, g, and h constants, and in this case, changing values of f parameter also only the maximum of α is modified. In Refs. 14 and 18, we have showed as a and b parameters are associated mainly to α-relaxation, c to β* and d to β. In the case of dielectric manifestation of viscoelasticity, we have demonstrated earlier[14,20] as f and e parameters are associated to α-relaxation, g to β*, and h to β.

In the next section, we present the experimental results obtained for PEN-films; this experimental data were studied on a fractional calculus approach using MFM and DFM.

EXPERIMENTAL MEASUREMENTS OF E^* AND ε_r^*

The PEN films used in this work were provided by Dupont de Nemours, Luxembourg. The as-received samples were PEN-films with 45 and 70 μm of thickness, of very low crystallinity ($\chi < 1\%$). PEN films, 70 μm thick, were used for DMA, and for dielectric relaxation spectroscopy (DRS), PEN films, 45 μm thick, were used. The amorphous structure of the as-received samples was modified by isothermal treatments to obtain a semicrystalline microstructure. Figure 9 shows DSC measurements for the as-received sample of PEN and for isothermal treated samples at 160°C at different times; the measurements were carried out using a TA Instruments DSC 2010 CE, between 30 to 300°C, and we used a temperature increase at a rate of 10°C/min. For the as-received samples of PEN (amorphous samples), the glass transition temperature is obtained at 124°C, the maximum of cold crystallization at 196°C and the melting temperature at 268°C. For the glass transition, the changes of ΔCp baseline become less pronounced

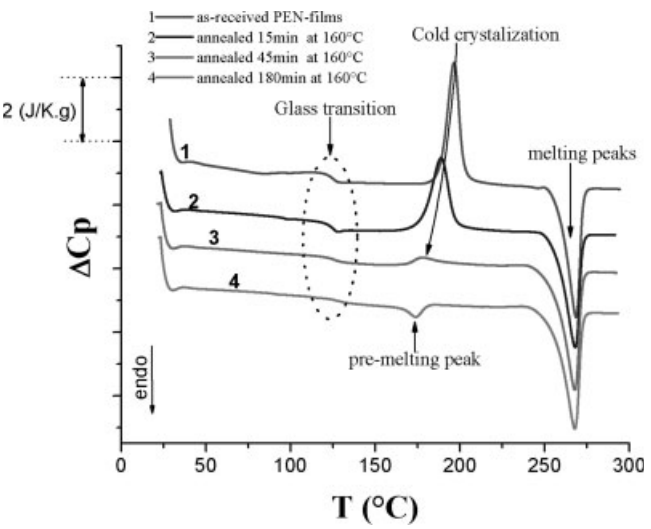

Figure 9 DSC measurements of the as-received and annealed samples of PEN at 160°C.

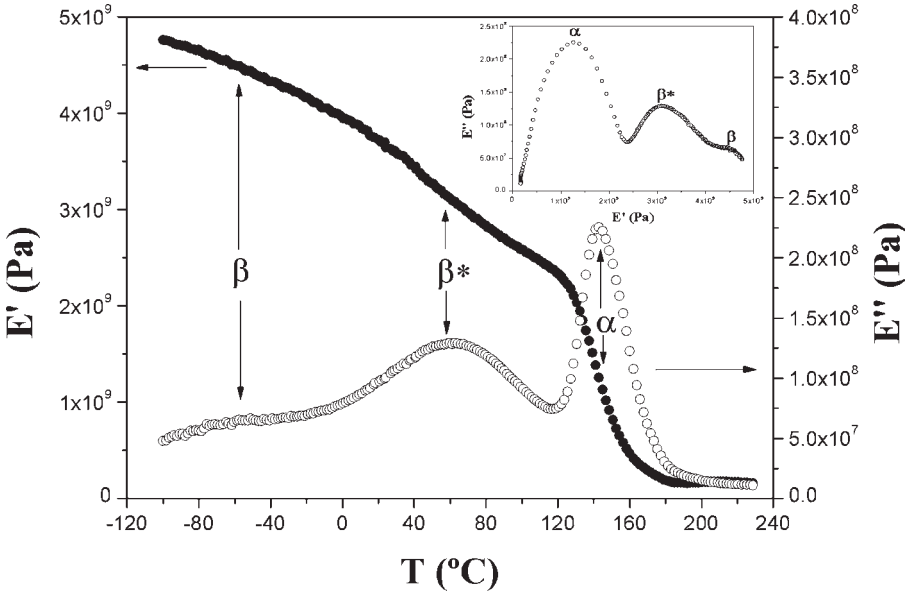

Figure 10 The experimental data for the real and imaginary parts of E^* at a frequency of 10 Hz, for a specimen annealed at 170°C/180min.

when the isothermal treatment times increases. A cold crystallization exothermic peak is clearly visible in the curve of as-received PEN sample. The amplitude of this exothermic peak decrease significantly when the thermal treatment times increases. For PEN-samples annealed during 180 min to 160°C, the cold crystallization peak is not detected and a small premelting peak is observed instead. These experimental results are in agreement with the results reported by several authors.[1,5–8] A more complete studied of relaxation phenomena can be obtained using DMA and DRS. The next section are experimental measurements of E^* and ε_r^* by DMA and DRS in a wide temperature range for several samples of PEN films.

Dynamic mechanical analyses

Several samples of PEN-films (70-μm thick) with different morphology were analyzed by DMA. The dynamic mechanical measurements were performed using a DMA 2980 TA instruments device. The measurements of E^* were made between −120°C and 230°C. We used a temperature increase at a rate of 2°C/min, for five different frequencies: 5, 10, 15, 20, and 25 Hz. The morphology of as-received samples of PEN was modified by isothermal treatments at 170°C for different times, obtaining specimens with different crystallinity, χ. The crystallinity rate of the as-received and annealed films was calculated as follows:

$$\chi(\%) = \frac{\Delta H_m - \Delta H_c}{\Delta H_f} \times 100 \qquad (23)$$

where ΔH_m and ΔH_c are the melting enthalpy and the crystallization exothermic enthalpy in the DSC diagrams (Fig. 9) and $\Delta H_f = 103.4\ J/g$ is the melting enthalpy of 100% crystalline PEN.[1,6]

Figure 10 shows the experimental data for the real and imaginary parts of E^* at a frequency of 10 Hz, for a specimen annealed at 170°C/180 min (χ = 44%). In $E''(T)$ diagram, we can identify the three PEN-relaxation peaks labeled: β, β*, and α, in order of increasing temperature. The β-mechanic relaxation is centered around −70°C. The β*-mechanic relaxation is centered around to 63°C, and the α-mechanic relaxation peak centered around 143°C. Compared to the α and β* relaxation, the intensity or the strength of the β process is quite low; in the redraw of Figure 10, we can clearly identify in the plan-complex the three maxima associates to mechanical relaxations of PEN, this graph is also named Cole–Cole diagram. Their molecular assignments have been discussed in detail previously.[1,5,7,8]

Figures 11(a and b) show the effect of morphology on the experimental data of the real an imaginary parts of E^* for specimens of PEN-films with different values of χ. Because of the isothermal treatments, the intensity of the β, β*, and α relaxations decreases because the content of the amorphous phase is decreased when the isothermal treatment times increases. The α-mechanical relaxation is the anelastic manifestation of the glass transition of PEN, the corresponding peaks of $E''(T)$ are accompanied by an important decrease in $E'(T)$ when temperature increases. For the short-time ($t < 120$ min) annealed samples, after passing through the glass transition, the amorphous PEN-phase begins to crystallize and

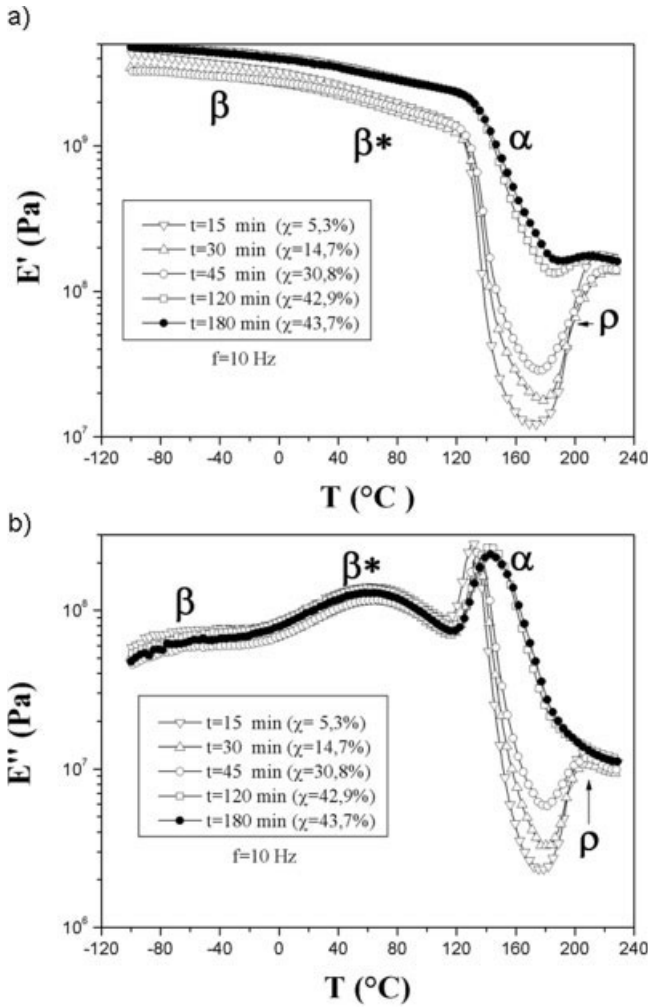

Figure 11 The effect of isothermal treatments on the experimental data of the real (a), and imaginary (b) parts of E^*.

a rapid increase in the storage modulus, E', can be observed above 180°C, this phenomenon is manifested as a decreases of the amplitude of ρ-peak in $E''(T)$ diagrams. In general, the shape of the experimental curves of $E'(T)$ and $E''(T)$ are modified when the isothermal treatment times increases. In the next section, we show as these experimental data can be described by our MFM.

Dielectric relaxation spectroscopy

The dielectric analysis was carried out in a temperature range from −100 to 200°C, at a heating rate of 2°C/min, for 12 different frequencies (1.2, 4.5, 10, 20, 45, 100, 200, 450, 10^3, 10^4, and 10^5 Hz). The device used is a dielectric analyzer of type DEA270-TA Instruments.

PEN films used in this part of work were samples of 45 μm thick with different crystallinity: 5.1, 20.1, 41.3, and 42.5% obtained at different times of isothermal treatments at 160°C from as-received PEN films (amorphous films).

The variations of the real and imaginary parts of ε_r^* at a frequency of 10 Hz are presented in Figure 12 for a specimen with $\chi = 42.5\%$ (isothermal treatment at 160°C/180 min). On the $\varepsilon_r''(T)$ diagram the presence of three peaks (β, β*, and α) are observed. The glassy low temperature peak β appeared around to −62°C, the glassy high temperature peak β* is centered around 70°C, and the high temperature relaxation α is displayed at 140°C. The α-peak is associated with dielectric manifestation of the glass transition. In the temperature range where β, β*, and α peaks

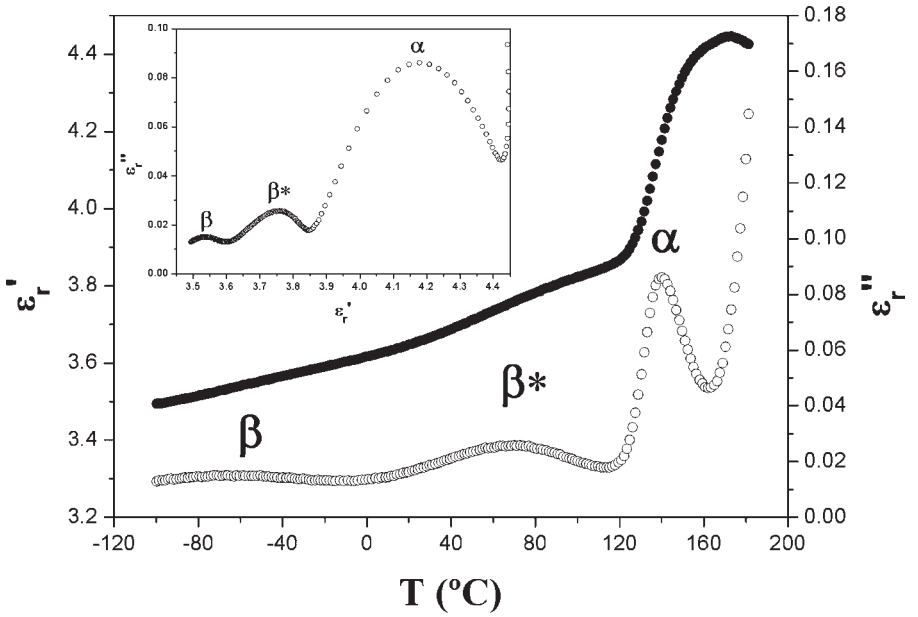

Figure 12 The experimental data for the real and imaginary parts of ε_r^* at a frequency of 10 Hz, for a specimen annealed at 160°C/180 min.

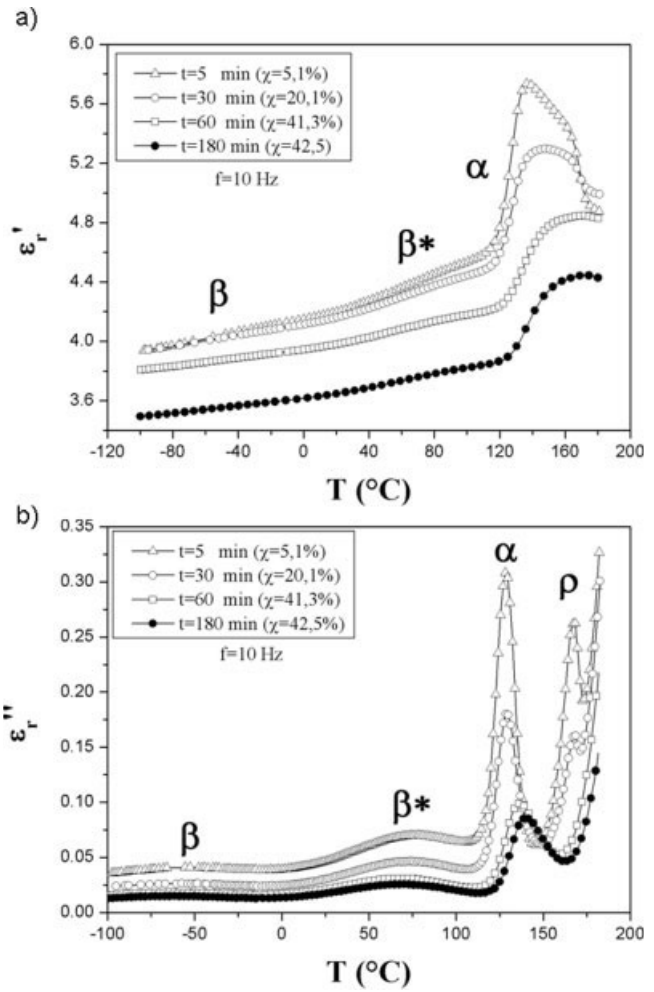

Figure 13 The effect of isothermal treatments on the experimental data of the real (a), and imaginary (b) parts of ε_r^*.

are displayed ε_r' presents ascending values when temperature increases. The redraw in Figure 12 shows as the Cole-Cole diagram (ε_r' and ε_r'' in the complex plan) presents the three peaks associated to β, β*, and α dielectric relaxations.

Figure 13(a and b) show the effect of morphology on experimental data of the real an imaginary parts of ε_r^* for specimens of PEN-films with different values of crystallinity. There is a global decreases in $\varepsilon_r'(T)$ diagram when the time of isothermal treatments increases. In the $\varepsilon_r''(T)$ diagrams, the amplitude of β, β*, and α peaks decrease when the time of isothermal treatments increases. The cold crystallization peak (ρ) is not detected in the PEN specimen annealed during 180 min at 160°C. The effect of electrical conductivity is present in all samples of PEN for $T > 170$°C, this effect is observed as an important increase in $\varepsilon_r''(T)$ when temperature increases.

Independently of the technique, the maxima of $E''(T)$ and $\varepsilon_r''(T)$ peaks associated with the α-relaxation are shifted toward higher temperatures, when the isothermal treatment times increases. On the other hand, both decreasing values of $\varepsilon_r'(T)$ and increasing values of $E'(T)$ are obtained, when the cold crystallization process take place. In general, the shape of the experimental curves of E^* and ε_r^* are modified when the time of the isothermal treatments increases.

In the next section, we will compare the theoretical predictions of the MFM and the DFM with experimental results of E^* and ε_r^* for PEN-samples with different crystallinity rates.

COMPARISON BETWEEN EXPERIMENTAL RESULTS AND THEORETICAL PREDICTIONS OF MFM AND DFM

We compared the theoretical predictions of MFM and DFM with the experimental results of the real and imaginary parts of E^* and ε_r^*, obtained under isochronal conditions at a frequency of 10 Hz. Figure 14(a and b) show the good agreement between theoretical and experimental isochronal spectra of the mechanical and dielectric relaxation phenomena for PEN-sample annealed at very long times (180 min), in a temperature range were β, β*, and α relaxation are displayed. Table I shows the values of fractional orders of spring-pots and cap-resistors and the activation parameters used to obtain the predictions of MFM and DFM of Figure 14(a and b). For the MFM, we obtain which $b > a > c > d$ and for the DFM, $f > e > g > h$. These parameters were calculated from experimental Cole–Cole diagrams as has been explained earlier.[14,18,20]

As a first approximation, the molecular motions associated with β-relaxation (mobility of the carbonyl groups of PEN chains) can be represented by parameter d in the case of the mechanical spectra, and for h in the case of dielectric spectra. The partially cooperative motions associated with β*-relaxation (mobility of the naphthalene groups) can be represented by parameter c for mechanical spectra and for g parameter in the case of dielectric spectra. Finally, parameters b and a could be used to represent the cooperative mechanical motions associated with α-relaxation, and the parameters f and e could be used to represent the cooperative dipolar movements associated with the dielectric manifestation of α-relaxation.

From the activation parameters shown in Table I, we can obtain the theoretical description of the temperature dependence of relaxation times (τ parameters) for each relaxation phenomenon for both the MFM and the DFM. Figure 15(a) shows experimental values of mechanical relaxation times and the theo-

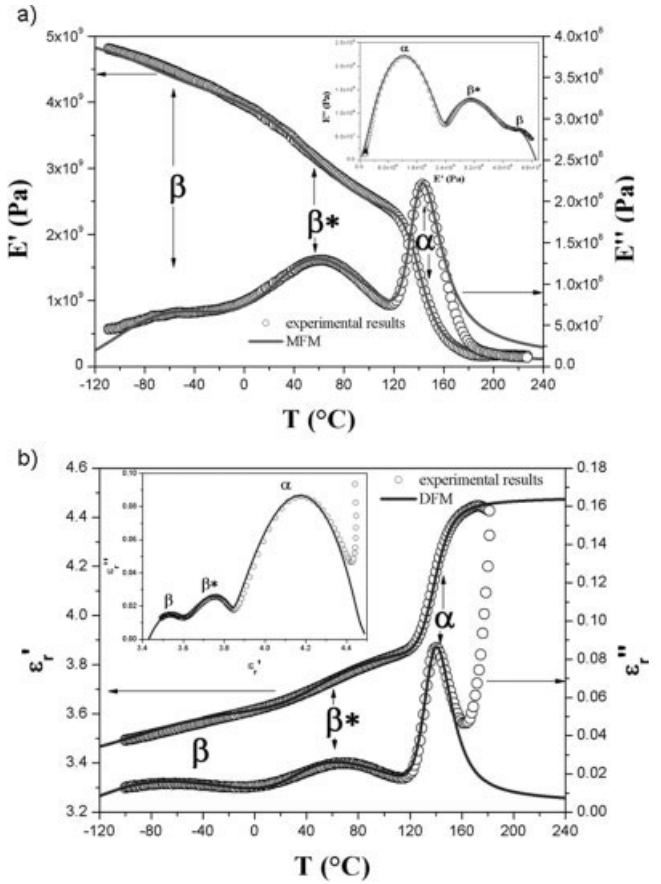

Figure 14 (a) Comparison between the experimental data and MFM-prediction of the isochronal behavior of the real and imaginary parts of E^*, for a semicrystalline PEN sample with 42% of crystallinity. (b) Comparison between the experimental data and DFM-predictions of the isochronal behavior of the real and imaginary parts of ε_r^*, for a semicrystalline PEN sample with 42% of crystallinity.

retical predictions of τ parameters for the MFM; we observed an excellent agreement between experimental data and theoretical descriptions. On the other hand, Figure 15(b) shows the comparisons between experimental data of τ for each dielectric relaxation and the theoretical descriptions of τ obtained from the activation parameters of the DFM.

In Table II, we present the MFM-parameters calculated for the description of the mechanical relaxation phenomena of PEN-samples annealed at different times. Table III shows the DFM-parameters calculated for the dielectric analysis of PEN-films annealed at different times. From Tables II and III we can point out that:

- The b and f parameters are very large affected for isothermal treatments, both parameters decreases when the amorphous phase decreases. However, a and e parameters are less affected for isothermal treatments. These four parameters are associated to cooperative molecular mobility of the α-relaxation. In the case of the mechanical manifestation of α, when the value of b parameter is close to 1 the molecular mobility reflects a macroscopic behavior similar to a dashpot and when b is close to 0 the molecular mobility similar to a resort behavior. For the dielectric manifestation of α, when the value of f parameter is close to 1 the molecular mobility reflects a macroscopic behavior similar to a resistor and when f is close to 0 the molecular mobility similar to a capacitor behavior.
- It can be seen that fractional order associated to molecular mobility of β*-relaxation, c and g parameters, are almost constant for all annealed samples of PEN. The fractional orders d and h,

TABLE I
The Parameters of the MFM and DFM

Relaxation phenomena	MFM parameters	DFM parameters
α (cooperative movements)	$a = 0.17$	$e = 0.24$
	$b = 0.27$	$f = 0.41$
	$E1_U - E1_0 = 1.96 \times 10^9$ Pa	$\varepsilon 1_{rs} - \varepsilon 1_{r\infty} = 0.58$
	$\tau_0 = 1 \times 10^{-18}$ s	$\tau_0 = 1 \times 10^{-14}$ s
	$E_{a\ \text{single-movement}} = 0.66$ eV	$E_{a\ \text{single-movement}} = 0.47$ eV
	$T^* = 267°C$	$T^* = 267°C$
	$T_0 = 77°C$	$T_0 = 76°C$
β* (partially cooperative movements)	$c = 0.142$	$g = 0.19$
	$E2_U - E2_0 = 1.64 \times 10^9$ Pa	$\varepsilon 2_{rs} - \varepsilon 2_{r\infty} = 0.25$
	$\tau_0 = 1 \times 10^{-34}$ s	$\tau_0 = 1 \times 10^{-14}$ s
	$E_{a\ \text{single-movement}} = 2.04$ eV	$E_{a\ \text{single-movement}} = 0.56$ eV
	$T^* = 267°C$	$T^* = 267°C$
	$T_0 = -238°C$	$T_0 = -83°C$
β (noncooperative movements)	$d = 0.13$	$h = 0.17$
	$E3_U - E3_0 = 1.35 \times 10^9$ Pa	$\varepsilon 3_{rs} - \varepsilon 3_{r\infty} = 0.24$
	$\tau_0 = 1 \times 10^{-18}$ s	$\tau_0 = 1 \times 10^{-14}$ s
	$E_{a\ \text{apparent}} = 0.715$ eV	$E_{a\ \text{apparent}} = 0.5$ ev

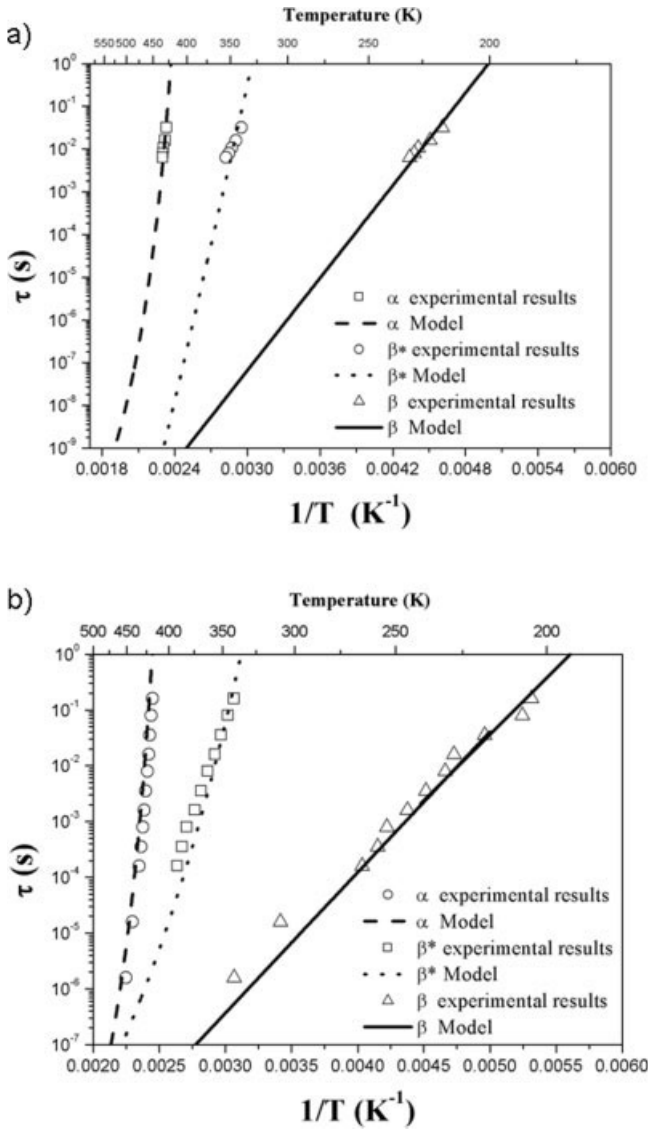

Figure 15 (a) Comparisons between experimental values of relaxation times and the theoretical predictions for mechanical relaxations. (b) Comparisons between experimental values of relaxation times and the theoretical predictions for dielectric relaxations.

which are associated to molecular mobility in β-relaxation practically, are not affected for the isothermal treatment times.

- The molecular mobility associated with the mechanical and dielectric manifestation of α-relaxation are cooperative processes in the temperature range from $T_0 = T_g$-50°C to $T^* = 267$°C, in this case, T^* is equal to the fusion temperature of PEN. These results are in agreement with the report of Rault[25] for several semicrystalline polymers.
- For β*-relaxation, the molecular movements are less cooperative than α-movements in the temperature range from $T_0 < T_g$-50°C to $T^* = 267$°C. However, the values of the activation parameters for the mechanical manifestation of β* are very different with respect the activation parameters of the dielectric manifestation of β*. For the mechanical β*-relaxation, τ_0 is very small than the characteristic times of the molecular vibrations (10^{-13} s), in addition the activation energy of the elementary movements of the partially cooperative mobility of β* is very large that the values associated to a potential energy barrier. This behavior can be associated to the presence of two kinds of molecular mobility of the naphthalene groups, the cis and trans configurations of the naphthalene groups.[1] So, the molecular mobility in β* induced by a mechanical stimulus is more complex which the β*-movements induced by an electrical stimulus. Hardy et al.[7,8] suggest that β*-relaxation should be assigned to the molecular fluctuations of aggregates of the naphthalene rings which have also been revealed by vibrational spectroscopy.[8]
- For β-relaxation, the apparent activation energies for both the MFM and DFM are of low value corresponding to noncooperative processes.

CONCLUSIONS

The real and imaginary parts of the mechanical and dielectric responses of PEN-films can be described by our fractional models (MFM and DFM) and the comparison between theory and experimental data over a wide range of temperature have been established by using DMA and DRS. The comparison between experimental results and theoretical predictions show good agreement and consequently a success for our MFM and DFM. We noted that the fractional orders (whose values are between 0 and 1) of both the spring-pots and the cap-resistors are related to molecular mobility associated with α, β*, and β relaxations. These fractional parameters can be considered as an indirect measured of the molecular mobility in each relaxation phenomena.

The parameters b and a represent the molecular mobility of the mechanical manifestation of the glass transition (relaxation α). On the other hand the noninteger orders f and e represent the molecular mobility of the dielectric manifestation of the glass transition.

For the β*-relaxation, the c parameter represents the molecular mobility of the mechanical manifestation β*, and g parameter is associated to the molecular mobility of the dielectric manifestation of β* process.

The localized molecular mobility of β-relaxation is associated to d parameter for the mechanical mani-

TABLE II
The Effect of Isothermal Treatments (at 170°C for PEN-Films of 70 μm Thickness) on the Parameters of the MFM

		Isothermal treatment times (min)				
Mechanical relaxations	MFM parameters	180	120	45	30	15
α (cooperative molecular mobility)	b	0.27	0.36	0.45	0.5	0.62
	a	0.17	0.17	0.16	0.16	0.17
	$(E1_U - E1_0)$	1.96×10^9 Pa	1.95×10^9 Pa	1.5×10^9 Pa	1.18×10^9 Pa	1.2×10^9 Pa
	E_a elementary movements (eV)	0.66	0.63	0.6	0.55	0.5
	T^* (K)	540	540	520	530	530
	T_0 (K)	350	350	350	350	350
	τ_0 (s)	1×10^{-18}	1×10^{-18}	1×10^{-18}	1×10^{-18}	1×10^{-18}
β* (partially cooperative motions)	c	0.142	0.148	0.14	0.14	0.14
	$(E2_U - E2_0)$	1.64×10^9 Pa	1.69×10^9 Pa	1.8×10^9 Pa	1.65×10^9 Pa	1.8×10^9 Pa
	E_a elementary movements (eV)	2.04	2.045	2.07	2.1	2.12
	T^* (K)	540	540	540	540	530
	T_0 (K)	35	35	35	40	35
	τ_0	1×10^{-34}	1×10^{-34}	1×10^{-34}	1×10^{-35}	1×10^{-21}
β* (no cooperative molecular motions)	d	0.13	0.13	0.135	0.13	0.13
	$(E3_U - E3_0)$	1.35×10^9 Pa	1.4×10^9 Pa	1.2×10^9 Pa	1.2×10^9 Pa	1.45×10^9
	E_a apparent (eV)	0.715	0.75	0.815	0.818	0.82
	τ_0	1×10^{-18}	1×10^{-18}	1×10^{-21}	1×10^{-21}	1×10^{-21}

TABLE III
The Effect of the Isothermal Treatments (at 160°C for PEN-Films of 45 μm Thickness) on the Parameters of the DFM

		Isothermal treatment times (min)			
Dielectric relaxations	DFM parameters	180	60	30	5
α (cooperative molecular mobility)	f	0.41	0.5	0.7	0.85
	e	0.24	0.23	0.31	0.36
	$\varepsilon 1_{rs} - \varepsilon 1_{r\infty}$	0.58	0.6	0.8	1.14
	E_a elementary movements (eV)	0.47	0.43	0.38	0.36
	T^* (K)	540	540	540	540
	T_0 (K)	349	350	350	350
	τ_0 (s)	1×10^{-14}	1×10^{-14}	1×10^{-14}	1×10^{-14}
β* (partially cooperative motions)	g	0.19	0.19	0.19	0.2
	$\varepsilon 2_{rs} - \varepsilon 2_{r\infty}$	0.25	0.29	0.44	0.57
	E_a elementary movements (eV)	0.56	0.57	0.59	0.61
	T^* (K)	540	540	540	540
	T_0 (K)	190	190	190	190
	τ_0 (s)	1×10^{-14}	1×10^{-14}	1×10^{-14}	1×10^{-14}
β (no cooperative molecular motions)	h	0.17	0.16	0.166	0.17
	$\varepsilon 3_{rs} - \varepsilon 3_{r\infty}$	0.24	0.29	0.4	0.49
	E_a apparent (eV)	0.5	0.51	0.52	0.53
	τ_0 (s)	1×10^{-14}	1×10^{-14}	1×10^{-14}	1×10^{-14}

festation of β, and h parameter represents the molecular motions of the dielectric manifestation of β.

The Fractional Calculus approach to the analysis of dynamic data (mechanical and dielectric experimental results) presented in this article shows the potential of the Fractional Calculus method to describe the isochronal specters of E^* and ε_r^* for polymer materials.

References

1. Zouzou, N. Thèse, Université Paul Sabatier, Toulouse, 2002.
2. Tonelli, A. E. Polymer 2002, 43, 637.
3. Higashioji, T.; Tsunekawa, T.; Bhushan, B. Tribol Int 2003, 36, 437.
4. Cañadas, J. C.; Diego, J. A.; Mudarra, M.; Belana, J.; Díaz-Calleja, R.; Sanchis, M. J.; Jaimés, C. Polymer 1999, 40, 1181.
5. Mayoux, C.; Martinez-Vega, J. J.; Guatavino, J.; Laurent, C. IEEE Trans Dielectr Electr Insul 2001, 8, 58.
6. Martinez-Vega, J. J.; Zouzou, N.; Boudou, L.; Guastavino, J. IEEE Trans Dielectr Electr Insul 2001, 8, 776.
7. Hardy, L.; Stevenson, I.; Fritz, A.; Boiteux, G.; Seytre, G.; Schönhals, A. Polymer 2001, 42, 5679.
8. Hardy, L.; Stevenson, I.; Fritz, A.; Boiteux, G.; Seytre, G.; Schönhals, A. Polymer 2003, 44, 4311.
9. Koeller, R. C. J Appl Mech 1984, 51, 299.
10. Bagley, R. L.; Torvik, P. J. J Rheol 1986, 30, 133.
11. Moshrefi-Torbati, M.; Hammond, K. J Franklin Inst 1998, 355B, 1077.
12. Novikov, V. U.; Kozlov, G. V. Russ Chem Rev 2000, 69, 523.
13. Carpinteri, A.; Cornetti, P. Chaos Solitons Fractals 2002, 13, 85.
14. Reyes-Melo, M. E. Thèse, Université Paul Sabatier, Toulouse, 2004. N° d'ordre:2004-T0U·0086–2.

15. Leyderman, A.; Qu, S.-H. Phys Rev E 2000, 62, 3293.
16. Alcoutlabi, M.; Martinez-Vega, J. J. J Macromol Sci Phys 1999, 38, 991.
17. Heymans, N. Signal Process 2003, 83, 2345.
18. Reyes-Melo, E.; Martinez-Vega, J.; Guerrero-Salazar, C.; Ortiz-Mendez, U. J Appl Polym Sci 2004, 94, 657.
19. Reyes-Melo, E.; Martinez-Vega, J.; Guerrero-Salazar, C.; Ortiz-Mendez, U. In: 8th International Conference on Solid Dielectrics (ICSD 2004), Toulouse, France, July 5–9, 2004.
20. Reyes-Melo, E.; Martinez-Vega, J.; Guerrero-Salazar, C.; Ortiz-Mendez, U. J Appl Polym Sci 2005, 28, 923.
21. Schiessel, H.; Blumen, A. J Phys A: Math Gen 1993, 26, 5057.
22. Heymans, N.; Bauwens, J. C. Rheol Acta 1994, 33, 210.
23. Hilfer, R., Ed. The Application of Fractional Calculus in Physics; World Scientific: Singapore, 2000.
24. Ngai, K. L. J Chem Phys 1998, 109, 6982.
25. Rault, J. J Non-Cryst Solids 2000, 271, 177.